Materials Today: Proceedings xxx (xxxx) xxx

Contents lists available at ScienceDirect

Materials Today: Proceedings

journal homepage: www.elsevier.com/locate/matpr

Design of a magnetically sensitive monotube damper for leg prostheses applying magnetic materials

Oscar Arteaga [a,*], Marcelo Ortiz [a], Eduardo Cárdenas [a], Juan Rocha-Hoyos [b], Katherine Amores [a], Andrés Balarezo [a], Jason A. Rodríguez [a]

[a] Universidad de las Fuerzas Armadas ESPE, Av. General Rumiñahui, Sangolquí 171103, Ecuador
[b] Universidad Internacional SEK Ecuador, Av. Río Amazonas, Quito 170515, Ecuador

ARTICLE INFO

Article history:
Received 12 July 2019
Received in revised form 29 August 2019
Accepted 2 September 2019
Available online xxxx

Keywords:
MR-fluids
Smart fluids
Magnetically responsive
Magnetic materials
Active damper

ABSTRACT

In this article, application of smart fluids in the design of a magnetorheological damper is presented, which consists of a semi-active suspension device whose operation is through a magnetorheological fluid to allow infinitely variable damping force control in real time over a wide range and low power requirements. The damper design presented in this investigation operates in valve and sheave modes. In addition, the properties of the materials were considered giving emphasis to the magnetic permeability. By means of the magnetic method of finite elements (FEMM), simulations were performed for the magnetic field analysis that occurs in the three coils. For the construction of the MR buffer, it was done in accordance with the results of the finite element simulation (FEA). It was implemented in a prototype of transfemoral prosthesis.

Selection and Peer-review under responsibility of the scientific committee of the First International Conference on Recent Advances in Materials and Manufacturing 2019.

1. Introduction

In the last twenty years, extensive research has been conducted on magnetorheological dampers, and different types of semi-active systems have been developed [1]. With the development of devices based on magnetorheological fluids [2], there is a way to counteract the problems of people with amputated limbs that are a direct consequence of illnesses, wars, accidents at work, traffic accidents and natural disasters, on a global scale it increases tens of thousands each year [3]. According to the World Health Organization, more than one billion people live around the world with some type of disability, approximately 15% of the world's population, a percentage that increases as the population ages and prevalence increases of chronic diseases [4].

The operation of magnetorheological fluids lies in stable suspensions of magnetizable micro particles dissipated in a carrier liquid such as silicone oil or water. Magnetorheological fluids possess rheological properties that can be controlled depending on the presence of a magnetic field [5]. The magnetorheological dampers have an important capacity to provide variable damping forces, also if any failure occurs the dampener can continue to operate, depending on the characteristics of the state of the fluid.

In several investigations such as El-Wahed and McEwan [6], Mazlan et al. the [7] and Mohd et al to the [8] presents the main applications for magnetorheological fluids, which can operate in flow mode, cut mode, valve mode and a combination of them. For all cases the fluid is located between two plates, but different operating conditions. For the flow mode, the resistance of the flow can be controlled by the magnetic field. In the cutting mode, the fluid is cut parallel to the plate that slides or rotates with respect to the other plate. For the compression mode, a force is applied to the plates in the same direction as a magnetic field and moved towards each other or separated from one another. Because each mode has its advantages and disadvantages, buffers were developed that use multiple modes of operation. Therefore, in this research, a magnetorheological damper with a combination of shear and valve was designed to prove that the combination of these two modes of work could also produce a high damping force.

2. Design of damper

Magnetorheological fluids MRF 140CG are free flowing liquids having a consistency similar to that of motor oil. However, in the

* Corresponding author.
E-mail address: obarteaga@espe.edu.ec (O. Arteaga).

https://doi.org/10.1016/j.matpr.2019.09.002
2214-7853/
Selection and Peer-review under responsibility of the scientific committee of the First International Conference on Recent Advances in Materials and Manufacturing 2019.

presence of an applied magnetic field, the particles align with the external field forming linear chains parallel to the field. This phenomenon restricts the fluid movement and the yield strength $\tau_{T(H)}$ is developed. The degree of change is related to the magnitude of the applied magnetic field, and can occur in only a few milliseconds. The Bingham plasticity model is effective at describing the essential field dependent fluid characteristic [9,10].

2.1. Characterization of MRF 140CG

The characterization of the magnetic material was performed according to DIN-53018, so, to determine the properties of MRF-140CG [11], see Fig. 1, different tests were performed on the fluid samples using a rotational rheometer Anton Paar Physica MCR-501, equipped with a magnetorheological cell MRD-70/1Text and a Julabo F-25 thermostatic bath system that allows to control the temperature of fluid samples with a stability less than ±0.1 °C. The tests of the fluid were performed under the following parameters:

Temperature: 20 °C, 30 °C, 40 °C and 50 °C
Magnetic field: 0 mT, 200 mT, 400 mT, 600 mT and 800 mT
Shear Rate: 0 to 350 rad/s

In Fig. 1(a), the flow curves of MRF-140CG for different shear rates are shown. Tests were performed in the absence of a magnetic field up to a maximum shear rate of 350 s^{-1} to avoid sample scatter. It is observed that the fluid presents a pseudo-plastic behaviour and that the shear stress increases with the increase of the shear rate. In Fig. 1(b), it can be seen that based on the Bingham plastic model, the resistance to flow increases as the intensity of the magnetic field increases, according to the regression Eq. (1), where, y represents the total yield strength of MRF-140CG in kPa, and x represents the magnetic flux density (B) in mT. The experimental data from the flow curves has been parameterized by fitting to each curve the Bingham rheological model, Eq. (1) [9], to experimental data.

$$y = 0.0556x - 0.7118 \tag{1}$$

$$\tau_{T(H)} = 0.0556 \cdot 1000 - 0.7118 = 54.896\text{kPa}$$

Due to the space and weight limitations of the leg prosthesis, it is considered to design an electromagnet that can generate a maximum magnetic flux density of 1.0 T, therefore, for 1000 mT the total yield strength developed by the MRF-140CG fluid in response to the applied field, is 54.896 kPa.

2.2. Dimensioning of the shock absorber

Based on the results obtained from the properties of the MRF 140CG, the dimensions and mass of the human body, the functional requirements of the shock absorber, the maximum allowable diameter of the shock absorber cylinder due to space restrictions in the leg prosthesis ($D_2 = 50mm$), the dimensions of the shock absorber and the flow channel h are determined, see Fig. 2, in order to guarantee an adequate range of shock absorption to be used in transfemoral prostheses, the calculations were made for different values of the design variables until the optimal dimensions, which comply with all the established functional parameters for the magneto-rheological dampers. To ensure that when the shock absorber is in the off-state, the person using the prosthesis remains stable when standing and supported with both legs [12], it is estab-

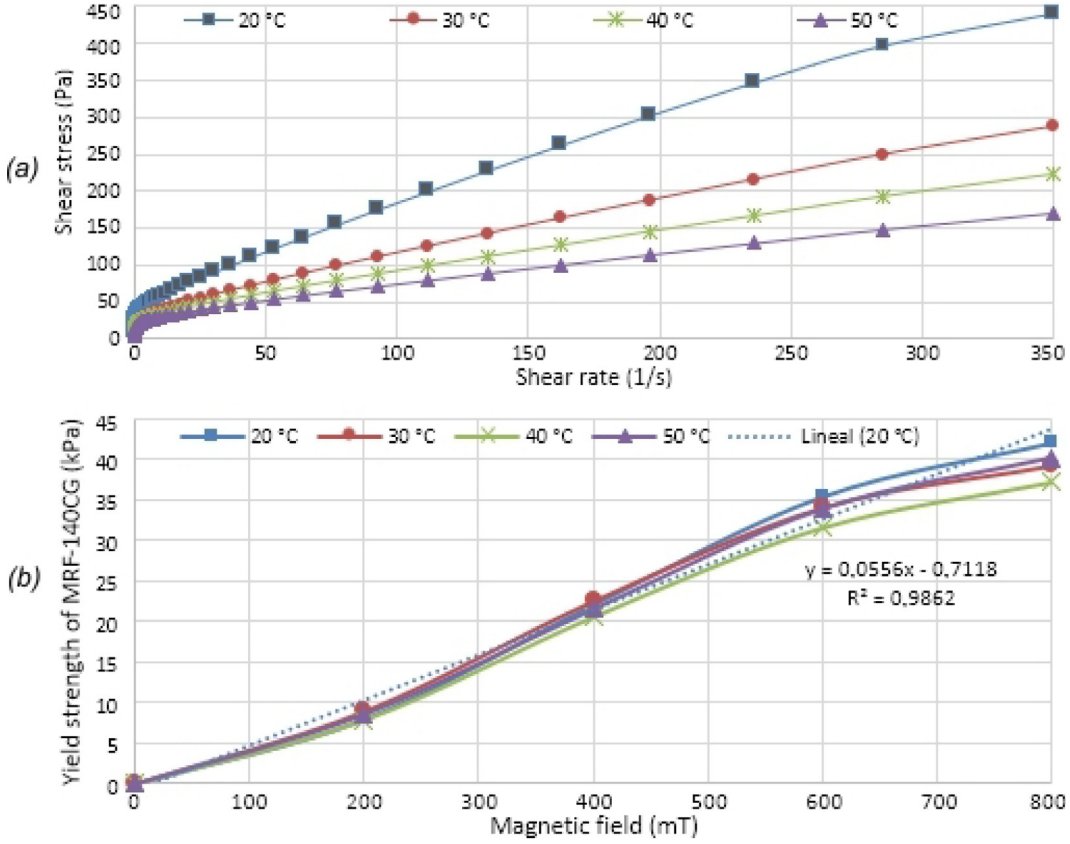

Fig. 1. Characteristics of the MRF-140CG oil-based MR fluids.

Please cite this article as: O. Arteaga, M. Ortiz, E. Cárdenas et al., Design of a magnetically sensitive monotube damper for leg prostheses applying magnetic materials, Materials Today: Proceedings, https://doi.org/10.1016/j.matpr.2019.09.002

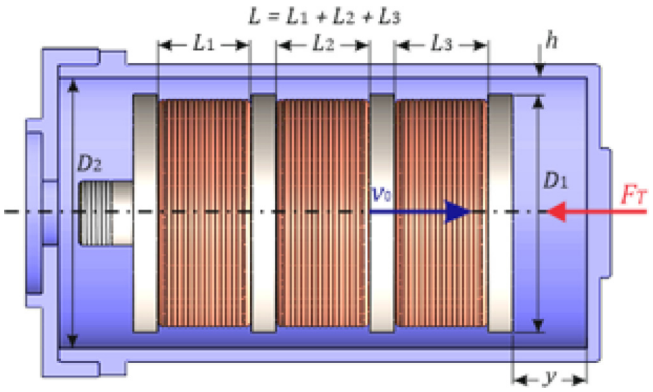

Fig. 2. Geometry proposed for the magnetorheological damper.

lished that the uncontrollable force required, must be equal to half the weight of a person with the 95th percentile, that is: $F'_{\eta} = 940/2 = 470\ N$. By means of spreadsheet the calculations are made for different values of the design variables. Next, the last 3 iterations are shown in Table 1, of which the optimum result was obtained with a flow channel thickness h = 0.7 mm.

2.3. Calculation of charges

In addition, the following variables are used to calculate the loads acting on the cylinder [13]: Non-controllable force F_{η}, controllable force $F_{\tau(H)}$, total force F_T, non-controllable pressure ΔP_{η}, controllable pressure $\Delta P_{\tau(H)}$, total pressureΔP, dynamic range λ_d. The uncontrollable force $F_{\eta} = 482.06N$ due to the viscous resistance of the fluid, is obtained from the following Eq. (1):

$$F_{\eta} = \left(1 + \frac{wh v_0}{2Q}\right) \frac{12\eta_p QL}{h^3 w} A_p \tag{2}$$

The coefficient c is calculated from Eq. (3):

$$c = 2.07 + \frac{1}{1 + \frac{0.4wh^2 \tau_{T(H)}}{12\eta_p Q}} \tag{3}$$

The controllable force $F_{\tau(H)}$ due to the shear stress induced by the applied magnetic field, is obtained from the Eq. (4):

$$F_{\tau(H)} = \frac{c\tau_{T(H)} L}{h} A_p = 5766.22\ N \tag{4}$$

The total force F_T developed by the magnetoreological absorber is:

$$F_T = 482.06 + 5766.22 = 6248.27\ N$$

The uncontrollable pressure ΔP_{η} due to the viscosity of the fluid, is obtained by means of Eq. (5):

$$\Delta P_{\eta} = \frac{12\eta_p QL}{h^3 w} = 0.2525\ \text{MPa} \tag{5}$$

The controllable pressure $\Delta P_{\tau(H)}$ due to the resistance to creep induced by the magnetic field, is obtained from Eq. (6):

$$\Delta P_{\tau(H)} = \frac{c\tau_{T(H)} L}{h} = 3.1083\ \text{MPa} \tag{6}$$

Then, the total pressure ΔP_T in the magnetorheological damper is: $\Delta P_T = 3.361$MPa, and the dynamic range of the device is calculated from Eq. (7).

$$\lambda_d = 1 + \frac{F_{\tau(H)}}{F_{\eta} + F_f} = 12.96 \tag{7}$$

This value is close to the optimum value of the dynamic range shown in [11]. Therefore, a wide range of control of the damping force is guaranteed and the sizing of the damper is validated.

The minimum volume of active fluid available V_d to generate the damping force is given by Eq. (8):

$$V_d = w \cdot L \cdot h = 1.84\ \text{cm}^3 \tag{8}$$

Because the total volume of fluid in a well-designed device must have 25 to 50 times the volume of active fluid, the appropriate range for the total volume of fluid in the buffer is:

$$46\ \text{cm}^3 \leq V_T \leq 92\ \text{cm}^3$$

Table 1
Spreadsheet used to find the optimum parameters configuration.

Design parameters	Nomenclature	Iterat.1	Iterat.2	Iterat.3
Diameter of shock absorber cylinder [m]	D_2	0.050	0.050	0.050
Diameter of the shock absorber piston [m]	D_1	0.046	0.0486	0.0488
Non-controllable force in the off-state [N]	F'_{η}	470.0	**470.0**	470.0
Thickness of annular flow channel – Gap [m]	h	0.0020	**0.0007**	0.0006
Equivalent width of the annular duct [m]	w	0.1508	0.1549	0.1552
Viscosity of the MRF-140CG in the off-state [Pa·s]	η_p	0.8081	0.8081	0.8081
Maximum damping length [m]	y	0.020	0.020	0.020
Time of the support phase in the walking cycle [s]	t	0.456	0.456	0.456
Average piston velocity [m/s]	v_0	0.0439	0.0439	0.0439
Area of the cross section of the piston [m^2]	A_p	0.0017	0.0019	0.0019
Effective area of fluid passage [m^2]	A_e	0.0003	0.0001	0.0001
Volumetric flow of the shock absorber [m^3/s]	Q	0.0001	0.0001	0.0001
Effective axial length of the magnetic pole [m]	L	0.4425	0.0166	0.0103
Average cutting area of the fluid [m]	A	0.0667	0.0026	0.0016
Parameter function of the velocity profile	c	2.1207	2.3913	2.4634
Controllable force dependent on the field [N]	$F_{\tau(H)}$	42808.24	5766.21	4355.42
Non-controllable force in off-state [N]	F_{η}	18.06	**482.06**	773.33
Total force developed by the shock absorber [N]	F_T	42826.30	6248.27	5128.75
Dynamic range	λ_d	2371.9195	12.9615	6.6320
Pressure due to yield strength resistance [Pa]	$\Delta P_{\tau(H)}$	2.58E + 07	3.11E + 06	2.33E + 06
Pressure due to the viscosity of the fluid [Pa]	ΔP_{η}	9.96E + 03	2.52E + 05	4.03E + 05
Total pressure in the shock absorber [Pa]	ΔP_T	2.58E + 07	3.36E + 06	2.73E + 06
Minimum volume of active fluid required [m^3]	V	3.185E − 03	1.702E − 06	5.705E − 07
Minimum volume of active fluid available [m^3]	V_d	1.335E − 04	1.843E − 06	9.621E − 07

Please cite this article as: O. Arteaga, M. Ortiz, E. Cárdenas et al., Design of a magnetically sensitive monotube damper for leg prostheses applying magnetic materials, Materials Today: Proceedings, https://doi.org/10.1016/j.matpr.2019.09.002

2.4. Solenoid design

For the design of the shock absorber, a concentric piston is considered in a cylinder which contains MR fluid and a cushion cylinder. The piston consists of three coils each with a length of 17 mm, with an outer diameter of 28.26 mm, which are wound in series on the outer piston diameter of the 48.6 mm. An advantage of the use of 5 different coils instead of simple coils lies in the fact that the remaining inductance of the circuit is smaller and, therefore, the reaction time is shorter [14] Taking into account that the piston of the shock absorber also complies. The functionality of the solenoid core, it is important the appropriate selection of an optimal material, which presents a high relative permeability, as well as a resistance to the flow to resist the stresses that are generated during the phases of damping. In this study, steel with a medium content of AISI 1020 carbon whose permeability was $\mu_r = 2000$ was selected as material. In the areas of shear and compression the size of the coils is dimensioned according to the highest values of magnetic field strength, H, which could be achieved by changing the applied current [15]. The cable selected for the coil is copper with a diameter of 0.8128 mm of type 20 AWG whose maximum current value is 1A, with a number of layers of 10 that is required to obtain 203 turns in each coil.

In order to check the parameters of the solenoid, it is analysed by means of an interactive finite element software (FEA) to simulate and solve three-dimensional (3D) electromagnetism problems. The boundary conditions assigned to perform the analysis are shown in Fig. 3 (a). The direction of the current is alternating in each coil so that the magnetic fields do not cancel each other out. This is done by winding the coils in the opposite direction. Fig. 3 (b) shows the distribution and direction of the magnetic field generated by the three coils of the solenoid. The highest field strength occurs in the solenoid core, mainly in the two central disks of the piston and its magnitude is 10108 T. Fig. 3 (c) shows the distribution of the magnetic field in 3D and determines that the field lines have a radial direction, in such a way that it is guaranteed that the magnetic field crosses the flow channel in a direction perpendicular to the flow of MRF-140CG along the entire outer circumference of each of the five semi-circular discs that make up the shock absorber piston.

2.5. Piston design

The piston, under critical operating conditions, must withstand the total damping force ($F_T = 6248.27N$) that is generated when the magnetic field is induced by 1.0 T. This force acts proportionally on the outer cylindrical surfaces of the four discs that make up the piston. The relative permeability of stainless steel AISI 316 is $\mu_r = 1.003$. The stress analysis of the piston is carried out by means of a finite element analysis software with a meshing with parabolic high-order tetrahedral solid elements, as shown in Fig. 4.

In the results of Fig. 5(a), it is observed that the maximum effort of Von Mises occurs in the hole for the passage of the winding wire and reaches a value of 254.81 MPa, however, since this effort is less that the resistance to creep of the AISI 1020 steel, the piston resists the maximum effort without failure. With respect to the distribution of the safety factor, in Fig. 5(b) it can be seen that the critical areas of the piston are in the hole for the winding cable and in the base of the circular discs of the piston, but as it is its minimum value 2.423, it is concluded that the design of the piston is safe and meets the resistance requirements under critical operating conditions.

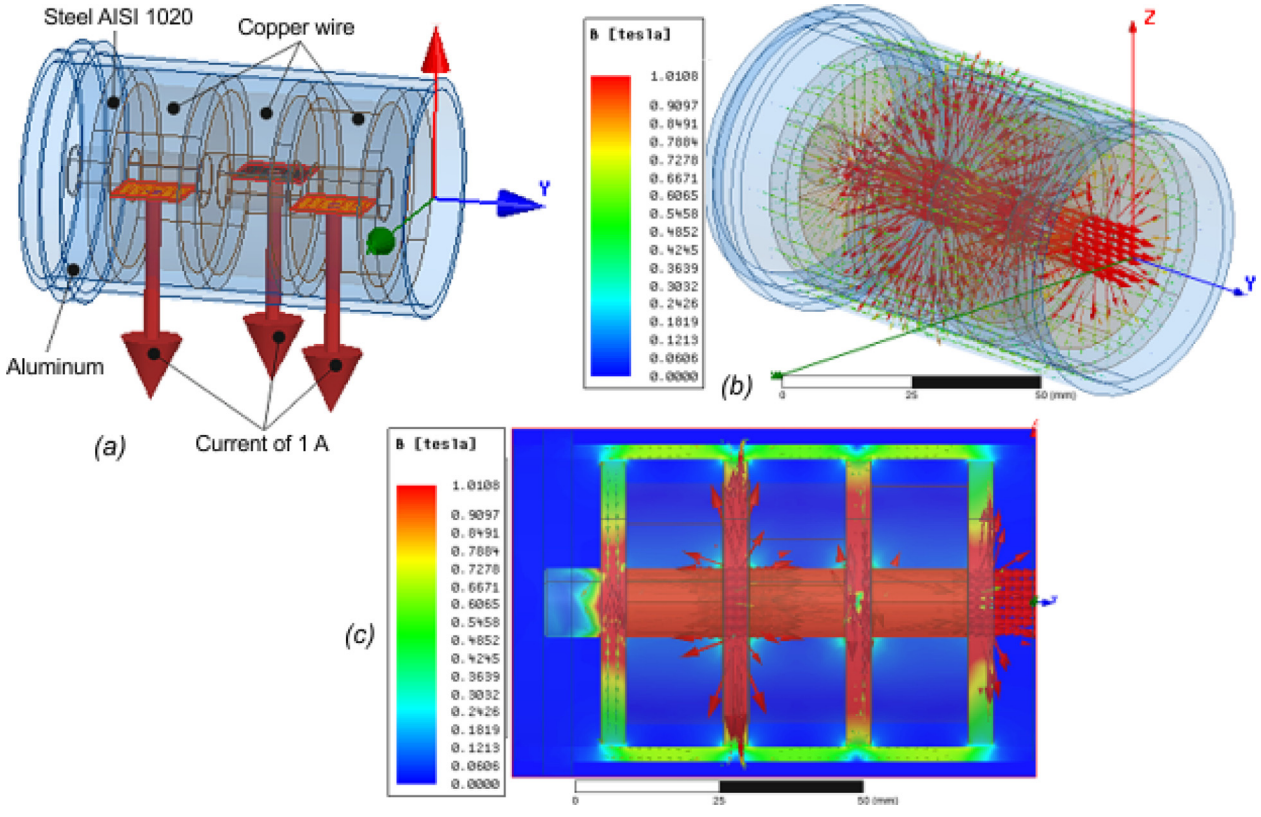

Fig. 3. Magnetic field analysis: (a) Boundary conditions for the analysis of electromagnetism; (b) Distribution and direction of the magnetic field in the YZ plane; (c) Distribution and direction of the magnetic field in 3D.

Please cite this article as: O. Arteaga, M. Ortiz, E. Cárdenas et al., Design of a magnetically sensitive monotube damper for leg prostheses applying magnetic materials, Materials Today: Proceedings, https://doi.org/10.1016/j.matpr.2019.09.002

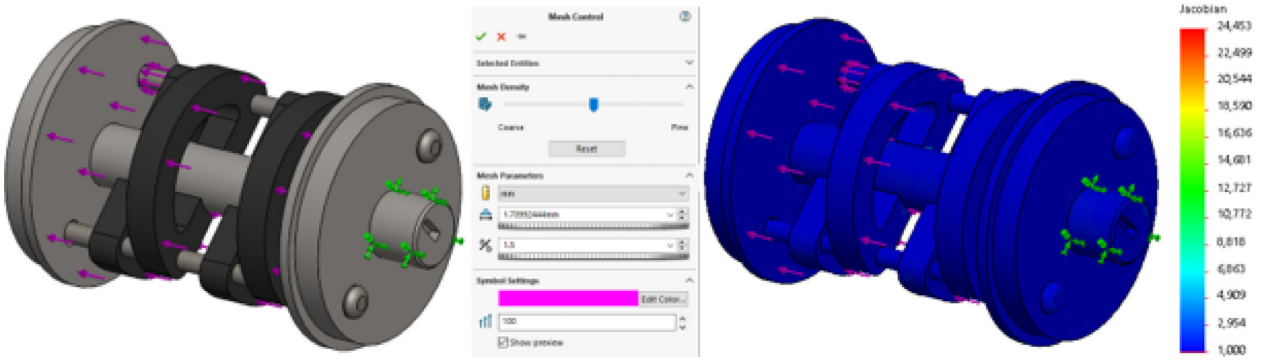

Fig. 4. Boundary conditions in the shock absorber piston and characteristics of the piston mesh.

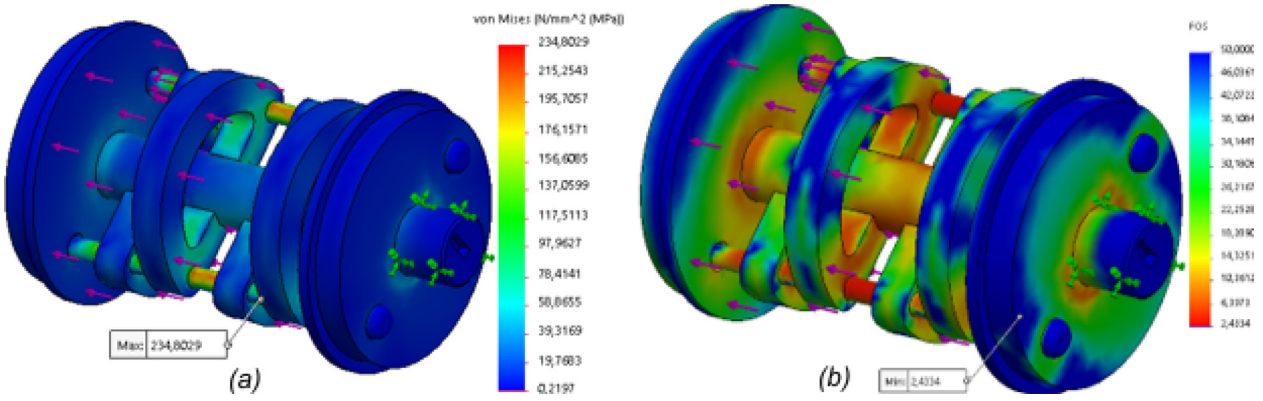

Fig. 5. (a) Distribution of efforts in the piston; (b) Distribution of the safety factor in the piston.

2.6. Cylinder design

With the purpose of reducing the weight of the shock absorber and at the same time guaranteeing its structural integrity and its proper functioning when the maximum damping loads are acting on it, the 7075-T6 aluminium alloy is used to manufacture the cylinder. The relative permeability of aluminium 7075-T6 is $\mu_r = 1.00002$. Under critical operating conditions, the cylinder must withstand the total pressure ($\Delta P_T = 3.361$ MPa) that is generated in the damper when the MRF-140CG fluid is under the action of a magnetic field of 1 T, this pressure acts on all the internal walls of the cylinder.

From the results of the stress analysis in the cylinder in Fig. 6(a), it can be seen that the maximum Von Mises stress has a value of 183.21 MPa and occurs at the base of the cylinder, however, this effort does not exceed the creep resistance of the material, so the cylinder does not fail. In the distribution of the safety factor shown in Fig. 6 (b), it can be seen that the critical areas are at the base of the cylinder, but since its minimum value is 2.76, the wall thickness of 2.5 mm is considered, it is suitable for the cylinder.

2.7. Assembly

Fig. 7 shows the 3D assembly of the main components of the magnetorheological damper prototype with the parts designed in the previous sections, then presents the built-in damper and is finally installed in a transfemoral prosthesis prototype with electronic components. necessary for its operation.

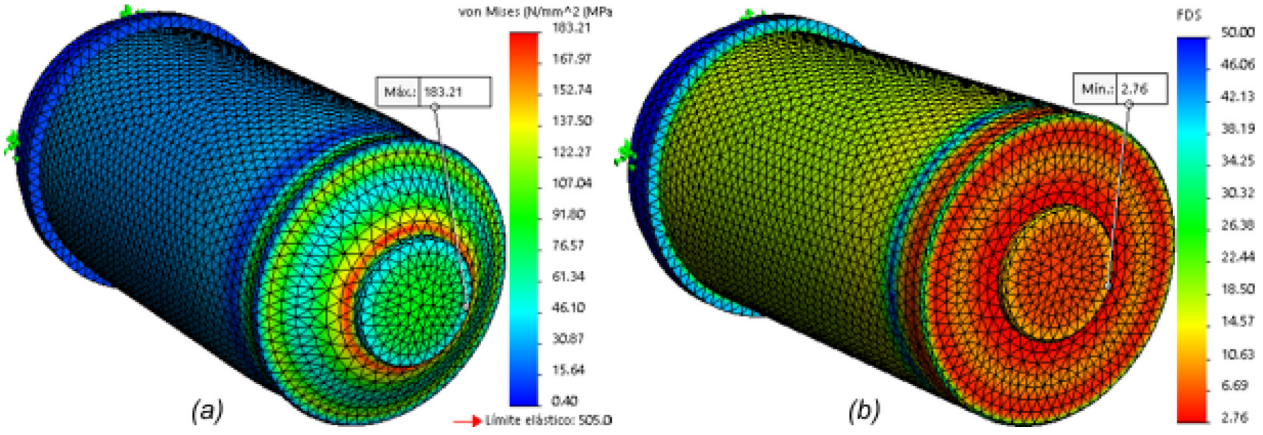

Fig. 6. (a) Distribution of efforts in the cylinder; (b) Distribution of the safety factor in the cylinder.

Please cite this article as: O. Arteaga, M. Ortiz, E. Cárdenas et al., Design of a magnetically sensitive monotube damper for leg prostheses applying magnetic materials, Materials Today: Proceedings, https://doi.org/10.1016/j.matpr.2019.09.002

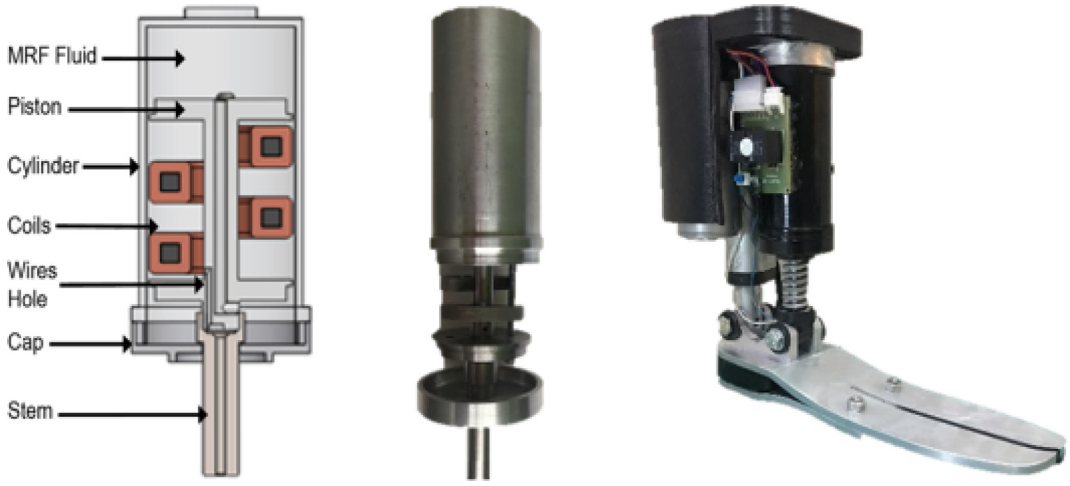

Fig. 7. Assembly of the prototype magnetorheological shock absorber.

3. Conclusions

The design of a magnetorheological shock absorber is investigated in this article. An analysis is carried out to determine the dimensions of the shock absorber and the flow channel in order to guarantee the adequate range for shock absorption. Engineering design calculations are derived from the loads acting on the cylinder. The parameters of length, outside diameter, number of coils, material for the solenoid, can be determined from the current equations, finally simulations of FEA and FEMM are shown to validate the design of the transfemoral prosthesis.

The results showed that the mixed mode damper MR has produced a unique damping characteristic where, in general, a greater damping force has been obtained in mixed mode than in simple mode reaching 6248.27 N.

The method of interaction of parameters using the calculation sheet is suitable for the design of cylinders according to the characteristics and parameters included in the model, so finite element simulations corroborate the calculated requirements.

References

[1] D. Wang, X. Bai, Smart Mater. Struct. 22 (2003) 075001.
[2] X. Zhu, X. Jing, L. Cheng, J. Intell. Material Syst. Struct. 23–8 (2013).
[3] H. Camacho, An. Fac. med. 71–4 (2010).
[4] World Health Organization, World Report Disability, 2011.
[5] J. Huang, J.Q. Zhang, Y. Yang, Y.Q. Wei, J. Mater. Process. Technol. 129 (2002).
[6] A. Wahed, C. Mcewan, J. Intell. Material Syst. Struct. 22–7 (2011).
[7] S. Mazlan, I. Ismail, H. Zamzuri, A. Ghani, J. Appl. Electrom. Mech. 36–4 (2011).
[8] I. Mohd, S. Mazlan, T. Kikuchi, H. Zamzuri, F. Imadduin, Mater. Des. 54 (2014).
[9] G. Yang, B.F. Spencer, J.D. Carlson, M.K. Sain, Eng. Struct. 20 (2002) 309–323.
[10] H. Fonseca, E. Gonzalez, J. Restrepo, C. Parra, C. Ortiz, IOP-J. Phys. 687 (2016) 01–04.
[11] O. Arteaga, M. Ortiz, E. Cardenas, S. Espin, M. Carvajal, H. Teran, M. Lara, IOP Conf. Ser.: Mater. Sci. Eng. 522 (2018), 01-05.
[12] V. Rajtukov, M. Michalíková, L. Bednarcíková, A. Balogová, J. Zivcak, Model. Mechan. Mechat. Syst. 96 (2014) 382–391.
[13] J. Goldasz, B. Sapiński, Insight into Magnetorheological Shock Absorbers, first., Springer, Bundesstadt, Switzerland, 2015.
[14] S. Kelso, Conf. Smart Struct. Mater. 4332 (2001).
[15] I. Mohd, S. Mazlan, H. Zamzuri, M. Mohd, S. Chuprat, Key Eng. Mater. 543 (2013).

Please cite this article as: O. Arteaga, M. Ortiz, E. Cárdenas et al., Design of a magnetically sensitive monotube damper for leg prostheses applying magnetic materials, Materials Today: Proceedings, https://doi.org/10.1016/j.matpr.2019.09.002